

Landmine Detection and Localization Using Chemical Sensor Array Processing

Aleksandar Jeremić, *Student Member, IEEE*, and Arye Nehorai, *Fellow, IEEE*

Abstract—We develop methods for automatic detection and localization of landmines using chemical sensor arrays and statistical signal processing techniques. The transport of explosive vapors emanating from buried landmines is modeled as a diffusion process in a two-layered system consisting of ground and air. Measurement and statistical models are then obtained from the associated concentration distribution. We derive two detectors (the generalized likelihood ratio (GLR) test and the mean detector) and determine their performance in terms of the probabilities of false alarm and detection. To determine the unknown location of a landmine, we derive a maximum likelihood (ML) estimation algorithm and evaluate its performance by computing the Cramér-Rao bound (CRB). The results are applied to the design of chemical sensor arrays, satisfying criteria specified in terms of detection and estimation performance measures and for optimally selecting the number and positions of sensors and the number of time samples. To illustrate the potential of the proposed techniques in a realistic demining scenario, we derive a moving-sensor algorithm in which the stationary sensor array is replaced by a single moving sensor. Numerical examples are given to demonstrate the applicability of our results.

Index Terms—Landmine detection, localization, moving sensor, sensor array processing.

I. INTRODUCTION

THE EXISTENCE of large numbers of landmines poses a severe threat to human life in many areas throughout the world. Some estimates of the total number of mines deployed is well above 100 million. However, methods for mine clearing have not evolved significantly in the past few decades. Several methods that are currently used for mine detection include manual prodding, metal detecting, applying mechanical techniques, and the use of trained animals. The only electronic equipment of widespread use is the traditional metal detector, which is reliable but not very efficient with respect to its false alarm rate. In addition, today's mines are often devoid of metal parts, making them invisible to the metal detector.

Current research on developing new technologies for mine clearing includes trace-explosive detection, ground-penetrating radar, magnetometers, advanced metal detectors, infrared and multispectral imaging, nuclear technology, nuclear quadrupole

resonance, passive millimeter wave detection, and acoustic methods [1].

Trace explosive detection is one of the most promising techniques since mines always contain explosive materials such as trinitrotoluene (TNT), cyclonite (RDX), and PET. It is therefore crucial to develop efficient methods for their detection and localization using chemical sensing. However, current research in this area has been mostly directed toward the development of new and enhancement of existing (in terms of sensitivity) chemical sensing techniques.

It is sometimes believed that automated systems based on current technologies cannot match the olfactory abilities of animals. Because of their keen sense of smell, dogs have a high degree of success in detecting mines. However, dogs require training and are sensitive to environmental conditions. More importantly, although they are quite effective at detection, their localization accuracy is usually poor [2]. Artificial odor or vapor sensing technologies such as chemoluminescence [3], [4], mass spectroscopy, and biosensing [5] also constitute valid techniques for detecting mines, but the *localization* of mines remains a challenging task.

In this paper (see also [6] and [7]), we present methods for automatic detection and localization of mines using measurements from a spatially distributed, cooperative array of chemical sensors, combined with optimal statistical signal processing techniques. We derive algorithms for detecting explosive vapors emanating from a landmine, estimating its location, and designing sensor arrays for optimum detection and estimation performance.

Our proposed methods have the following advantages over gradient-based methods, animals, and animal-emulation detection mechanisms.

- 1) By using an array of sensors that make measurements over a period of time, spatial and temporal information in the source locale is fully utilized.
- 2) Sensors act cooperatively by sharing this information, thereby utilizing it in an optimal manner.
- 3) The system parameters and processing techniques can be optimized for particular scenarios.
- 4) Predictable performance enables optimal selection of sensor array parameters.
- 5) By using vapor transport models, we can account for local minima and maxima in concentration levels (resulting from a spatially dependent diffusivity, for example) that could confuse gradient-following or animal-emulation systems [8]; however, in the present study, we do not consider the ability of our method to deal with such a scenario.

Manuscript received June 8, 1999; November 5, 1999. This work was supported by the Air Force Office of Scientific Research under Grants F49620-97-1-0481 and F49620-99-1-0067, the National Science Foundation under Grant MIP-9615590, and the Office of Naval Research under Grant N00014-98-1-0542. The associate editor coordinating the review of this paper and approving it for publication was Prof. A. M. Zoubir.

The authors are with the Department of Electrical Engineering and Computer Science, The University of Illinois at Chicago, Chicago, IL 60607-7053 USA (e-mail: ajeremic@eecs.uic.edu; nehorai@eecs.uic.edu).

Publisher Item Identifier S 1053-587X(00)03292-X.

In Section II, we develop a mathematical model for the spatial and temporal evolution of landmine vapor concentration distribution in the ground and in the air. Using this model, in Section III, we derive a spatio-temporal measurement model for the chemical sensor array, assuming that the sensors are selective to a particular explosive. We also derive a parametric statistical model for the array's measurements as a function of the source and medium parameters. Using this model, we develop a maximum likelihood (ML) estimator to find the mine location. We evaluate the performance of the proposed estimator by comparing it with the Cramér-Rao bound [9], which determines the optimal accuracy for the system (and unbiased estimators). We develop a detection algorithm based on the generalized likelihood ratio (GLR) test [10] and evaluate its performance by calculating probabilities of detection and false alarm. In Section IV, we propose methods for optimum array design, including choice of number of sensors and time samples, and sensor positions. In Section V, we present a localization algorithm in which the stationary sensor array is replaced by a single moving sensor. Section VI demonstrates the applicability of our results with numerical examples. In Section VII, we propose possible extensions of our algorithms to the more realistic case of a distributed source. Concluding remarks are given in Section VIII.

The proposed approach extends our previous work in [11]–[13].

II. PHYSICAL MODELING

In this section, we derive a physical model of explosive vapor transport in ground and air corresponding to vapor emission from landmines. The transport is mathematically described as a diffusion process by appropriate differential equations to which other effects are added.

Landmines and shallow, buried, unexploded ordnance (UXO) have chemical signatures consisting of explosive vapors such as TNT, RDX, and PET. Therefore, they can be considered to be vapor-emitting, underground chemical sources. Once released, the vapors are transported by phenomena such as molecular diffusion, advective processes, and turbulence. By modeling the vapor concentration distribution as a function of mine location and solving the inverse problem, we can detect and localize landmines and UXO.

To model the environment, we use a simplified system of two homogeneous, isotropic, infinite layers: ground ($z < 0$, layer 1) and air ($z > 0$, layer 2). Let $c_1(\mathbf{r}, t)$ and $c_2(\mathbf{r}, t)$ denote the vapor concentration in ground and air, respectively, in units of cubic kilograms per meter at location $\mathbf{r} = [x, y, z]^T$ and time t . The diffusion model is given by the following system of differential equations

$$\begin{aligned} \frac{1}{\kappa_1} \frac{\partial c_1(\mathbf{r}, t)}{\partial t} &= \nabla^2 c_1(\mathbf{r}, t) \\ \frac{1}{\kappa_2} \frac{\partial c_2(\mathbf{r}, t)}{\partial t} &= \nabla^2 c_2(\mathbf{r}, t) - \nabla[c_2(\mathbf{r}, t)\mathbf{v}(t)] \end{aligned} \quad (2.1)$$

where κ_1 and κ_2 are the effective ground and air diffusivities respectively, and $\mathbf{v}(t)$ is the wind velocity. Note that (2.1) incorporates turbulent diffusion in air and the effect of ground porosity

by approximating them as molecular diffusion processes with larger diffusivities κ_1 and κ_2 ; see [14].

The spatio-temporal distribution of the vapor concentration is uniquely determined by (2.1) and the following limiting conditions:

$$c_1(x, y, 0, t) = c_2(x, y, 0, t) \quad (2.2)$$

$$f_1(x, y, 0, t) = f_2(x, y, 0, t) \quad (2.3)$$

where $f_i(x, y, 0, t)$, ($i = 1, 2$) represents the unknown flux density at the boundary between the ground and air, i.e., $f_i(x, y, 0, t) = \kappa_i(\partial c_i/\partial z)|_{z=0}$.

Condition (2.2) requires that the concentration distribution be continuous at the ground-air boundary. Condition (2.3) requires that the vapor flux in the z direction be the same on both sides of the boundary. Following [15], we assume that c_1 and c_2 are functions for which Fourier transforms with respect to the spatial coordinates exist.

To solve (2.1), we first transform $c_1(\mathbf{r}, t)$ and $c_2(\mathbf{r}, t)$ using the following transformation:

$$C_1(\omega, t) = \int_{-\infty}^{\infty} \int_{-\infty}^{\infty} \int_0^{\infty} c_1(x, y, z, t) e^{-i(x\omega_x + y\omega_y)} \times \cos(\omega_z z) dz dy dx \quad (2.4)$$

where $\omega = [\omega_x, \omega_y, \omega_z]^T$. Transformation (2.4) is a commonly used technique for solving diffusion equations when the boundary conditions are prescribed in one of the coordinate planes. The expression for $C_2(\omega, t)$ is of the same form but with different limits of integral for the z coordinate and is therefore omitted.

We can now solve (2.1) by applying the transformation in (2.4) to (2.1). Let $F(\omega, t) = \int_{-\infty}^{+\infty} \int_{-\infty}^{+\infty} f(x, y, 0, t) e^{-w_x x - w_y y} dy dx$ be the two-dimensional (2-D) Fourier transform of $f(x, y, 0, t)$ with respect to the spatial coordinates. Consequently, (2.1) becomes

$$\frac{1}{\kappa_2} \frac{dC_2(\omega, t)}{dt} = [||\omega||^2 - i\omega^T \mathbf{v}(t)] C_2 + F(\omega, t) \quad (2.5)$$

where $\mathbf{v}(t) = [v_x(t), v_y(t), v_z(t)]^T$ is the wind velocity.

We assume that the distances at which the measurements are taken are much larger than the source (mine) dimensions and, hence, use a point-source model (typical landmine dimensions range from 2 cm to 70 cm.) Thus, to solve (2.1), we first consider an instantaneous point-source located in the ground at \mathbf{r}_0 emitting vapors with strength μ and at time t_0 . The release rate of this source is given by $\mu\delta(t) = \mu\delta(\mathbf{r} - \mathbf{r}_0)\delta(t - t_0)$, where δ denotes the Dirac function, and μ is the strength of instantaneous source in units of kilograms per second. In addition, we assume that the wind velocity is constant in time. Obviously, this is an approximation that becomes more accurate if the average wind velocity is used. Then, the solution to (2.5) is given by

$$\begin{aligned} C_2(\omega, t) &= \mu \exp\{-\kappa_2[||\omega||^2 - i(\omega^T \mathbf{r}_0 + \omega^T \mathbf{v})]t\} \\ &+ \int_{t_0}^t \exp\{-\kappa_2[||\omega||^2 - i(\omega^T \mathbf{r}_0 + \omega^T \mathbf{v})]t'\} \\ &\times F(\omega, t - t') dt'. \end{aligned} \quad (2.6)$$

Thus, for an instantaneous source, the concentration distribution in air is given by the corresponding Green's function, which we obtain by applying the inverse transform to (2.6) to yield

$$c_2(\mathbf{r}, t) = \mu w_2(\mathbf{r}, t) + \int_{t_0}^t w_2(\mathbf{r}, t') * f(x, y, 0, t - t') dt' \quad (2.7)$$

$$w_2(\mathbf{r}, t) = \frac{\mu}{4\pi\kappa_2 t^{3/2}} \exp\left\{-\frac{\|\mathbf{r} - \mathbf{v}t - \mathbf{r}_0\|^2}{4\kappa_2 t}\right\} \quad (2.8)$$

and “*” denotes spatial convolution. To determine the function $c_1(\mathbf{r}, t)$, we first transform the domain $(-\infty < x < \infty, -\infty < y < \infty, 0 < z \leq +\infty)$ to $(-\infty < x < \infty, -\infty < y < \infty, -\infty < z \leq 0)$. We obtain $c_1(\mathbf{r}, t)$ by substituting $z' = -z$ and computing $c_2(x, y, -z', t)$, using the same operations that were used to compute (2.7). Thus, we have

$$c_1(\mathbf{r}, t) = \mu w_1(\mathbf{r}, t) + \int_{t_0}^t w_1(\mathbf{r}, t') * f(x, y, 0, t - t') dt' \quad (2.9)$$

$$w_1(\mathbf{r}, t) = \frac{\mu}{4\pi\kappa_1 t^{3/2}} \exp\left\{-\frac{\|\mathbf{r} - \mathbf{r}_0\|^2}{4\kappa_1 t}\right\}. \quad (2.10)$$

Let $h_i(\mathbf{r}, t) = w_i(\mathbf{r}, t)t^{3/2}/\mu$, for $i = 1, 2$. Then, the unknown flux density $f(x, y, 0, t)$, is computed using the boundary condition (2.2). We have

$$w(\mathbf{r}, t) = \int_{t_0}^t \frac{(h_1(\mathbf{r}, t') + h_2(\mathbf{r}, t')) * f(x, y, 0, t')}{(t - t')^{3/2}} dt' \quad (2.11)$$

$$w(\mathbf{r}, t) = w_1(\mathbf{r}, t) + w_2(\mathbf{r}, t). \quad (2.12)$$

Equation (2.12) is an Abel integral equation with respect to $f(x, y, 0, t)$ whose solution is given by

$$f(x, y, 0, t) = \mathcal{F}^{-1} \left\{ \frac{1}{\mathcal{F}[h_1(\mathbf{r}, t) + h_2(\mathbf{r}, t)]} \times \mathcal{F} \left[\frac{1}{\pi} \frac{d}{dt} \int_{t_0}^t \frac{w_1(\mathbf{r}, t') + w_2(\mathbf{r}, t')}{(t - t')^{3/2}} dt' \right] \right\}. \quad (2.13)$$

The solutions (2.7) and (2.9) can be interpreted as the response function for an instantaneous source. We can therefore obtain the concentration distribution for a continuous source by convolving (2.9) with the release rate. This convolution can be computed analytically in special cases, such as when the release rate is constant.

We are interested in two scenarios associated with the mine-localization problem. In the first scenario, we consider the case of induced emission of vapors. After a considerable period of time, underground mines no longer release significant amounts of vapor; hence, the concentrations may not be detectable. It has recently been proposed that this problem may be circumvented by inducing the evaporation of explosive molecules using microwaves, thus permitting the detection of long-buried ordnance

[2]. For this scenario, we model the release rate using an instantaneous source so that the concentration distribution is given by (2.7) and (2.9). The second is based on a quasistatic approach in which we assume that the mine has been buried for a sufficiently long time, hence, making concentration changes (with respect to time) negligible. Here, the concentration distribution can be obtained as the limit of (2.7) and (2.9) as $t \rightarrow \infty$ with $\mu(t) = \mu\delta(\mathbf{r} - \mathbf{r}_0)$, where μ is the source intensity in units of kilograms.

III. MINE DETECTION AND PARAMETER ESTIMATION

A. Measurement Model

We assume that the vapor concentration is sampled in time and space by an array of chemical sensors that are selective, i.e., they react to a single chemical substance in the presence of many other compounds. Thus, we suppose a spatially distributed array of m chemical sensors, possibly moving, takes measurements at points $\{\mathbf{r}_{i,j}, 1 \leq i \leq m, 1 \leq j \leq p\}$ and times t_j , where p is the number of time samples. The response of each sensor is modeled by

$$y(\mathbf{r}_{i,j}, t_j) = c(\mathbf{r}_{i,j}, t_j) + e(\mathbf{r}_{i,j}, t_j) \quad (3.1)$$

where $c(\mathbf{r}_{i,j}, t_j)$ denotes the vapor concentration of interest, and $e(\mathbf{r}_{i,j}, t_j)$ denotes measurement noise resulting from sensor noise, imperfect modeling, and nonideal selectivity. For the remainder of the paper, we will assume that the sensors' sensitivity threshold is sufficiently small, so as to have a negligible effect on detection performance.

B. Statistical Model

We lump the measurement model (3.1) into the following form:

$$\mathbf{y} = \mathbf{a}(\theta)\mu_0 + \mathbf{e} \quad (3.2)$$

where

\mathbf{y}	(mp) -dimensional measurement vector;
$\mathbf{a}(\theta)$	source-to-sensor transfer vector based on the diffusion model (2.9);
θ	vector of unknown source and medium parameters (mine location, starting time of diffusion, diffusivities and wind velocity);
μ_0	unknown source intensity;
\mathbf{e}	vector of measurement noise.

The $[i + (j - 1)m]$ th element of the vector $\mathbf{a}(\theta)$ is the vapor concentration at the location $\mathbf{r}_{i,j}$ and time t_j . The exact expression depends on the source model type: induced or continuous. For example, in the case of the induced emission using (2.9), in terms of the dimensionless coordinates

$$z'_{i,j} = -\frac{z_{i,j}}{[\kappa_1(t_j - t_0)]^{1/2}}$$

$$z'_0 = \frac{z_0}{[\kappa_1(t_j - t_0)]^{1/2}}$$

$$r'_{i,j} = \frac{r}{[\kappa_1(t_j - t_0)]^{1/2}}$$

this entry would be [7]

$$a_{i+(j-1)m}(\theta) = \frac{\kappa^2}{8\pi^2\kappa_1 t_j^{\frac{3}{2}}} \int_0^1 q_r(r'_{i,j}, u) \cdot q_z(z'_{i,j}, z'_0, \kappa, u) du \quad (3.3)$$

$$+ \frac{1}{\sqrt{\kappa_1\pi}} \int_{t_0}^{t_j} \frac{f(r, t)}{(t_j - t)^{\frac{3}{2}}} q_z\left(0, z'_0, \kappa, \frac{t}{(t_j - t_0)}\right) dt \quad (3.4)$$

where $\kappa = \kappa_1/\kappa_2$ and

$$\begin{aligned} q_r(r'_{i,j}, u) &= \frac{\exp[-\kappa^2 r'^2_{i,j}/4(\kappa^2 u + 1 - u)]}{(\kappa^2 u + 1 - u)u^{\frac{1}{2}}(1 - u)^{\frac{1}{2}}} \\ q_z(z'_{i,j}, z'_0, \kappa, u) &= \frac{\kappa z'_{i,j}(1 - u) + \kappa^3 u z'_0}{(1 - u + \kappa^2 u)^2} \exp\left\{-\frac{z'^2_0(1 - u) + \kappa^2 z'^2_{i,j} u}{4u(1 - u)}\right\} \\ &+ \frac{\kappa\pi^{\frac{1}{2}} u^{\frac{1}{2}}(1 - u)^{\frac{1}{2}}}{(1 - u + \kappa^2 u)^{\frac{3}{2}}} \left\{1 - \frac{\kappa^2(z' - z'_0)^2}{2(1 - u + \kappa^2 u)}\right\} \\ &\times \operatorname{erfc}\left\{\frac{(1 - u)z'_0 + \kappa^2 z'_{i,j}}{2u^{\frac{1}{2}}(1 - u)^{\frac{1}{2}}(1 - u + \kappa^2 u)^{\frac{1}{2}}}\right\} \\ &\times \exp\left\{-\frac{\kappa^2(-z'_{i,j} + z'_0)^2}{4(1 - u + \kappa^2 u)}\right\} \end{aligned} \quad (3.5)$$

and $f(r, t)$ corresponds to the flux density $f(x, y, 0, t)$ given by

$$f(r, t) = \frac{1}{\pi} \frac{d}{dt} \int_0^t \frac{g(r, \tau)}{(t - \tau)^{\frac{3}{2}}} d\tau \Big|_{t=t_j-t_0} \quad (3.6)$$

$$\begin{aligned} g(r, \tau) &= \frac{\kappa_2}{\left(\kappa_1^{\frac{3}{2}} + \kappa_2^{\frac{3}{2}}\right)\sqrt{\tau}} q_r\left(r'_{i,j}, \frac{\tau}{\kappa_1(t_j - t_0)}\right) \\ &\cdot q_z\left(z'_{i,j}, z'_0, \kappa, \frac{\tau}{\kappa_1(t_j - t_0)}\right). \end{aligned} \quad (3.7)$$

We will assume that the noise in (3.2) is uncorrelated in time and space, and Gaussian-distributed, with zero mean and unknown variance σ^2 . Note that since the concentration has a non-negative value, the Gaussian assumption is only an approximation that becomes more accurate as the signal-to-noise ratio (SNR) increases. We define the SNR as the ratio of the squared peak value of the concentration distribution to the noise variance.

For the remainder of the paper, we will consider the case of known medium parameters. These include the effective diffusivities of ground and air, with wind velocity \mathbf{v} , since they can be easily measured. Therefore, the dimension of unknown vector θ is 3 (unknown location). Observe that in the quasistatic model, the concentration distribution does not depend on t_0 . In the case of induced emission, t_0 is known and can be arbitrarily set to 0.

C. Parameter Estimation

To estimate the unknown source parameters, we use the ML estimator, which maximizes the function

$$l(\mathbf{y}, \theta, \mu) = (2\pi\sigma^2)^{-mp/2} \exp\left[-\frac{1}{2\sigma^2}\|\mathbf{y} - \mathbf{a}(\theta)\mu\|^2\right]. \quad (3.8)$$

This estimator is optimal in the sense that for a sufficiently large number of measurements, it achieves the best possible accuracy for unbiased estimators given by the Cramér-Rao bound [16]. The ML estimates $\hat{\theta}$, $\hat{\mu}$, and $\hat{\sigma}^2$ are given by [9]

$$\begin{aligned} \hat{\theta} &= \arg \max \left\{ \frac{\mathbf{y}^T \mathbf{y}}{\mathbf{a}^T(\theta)\mathbf{a}(\theta)} \right\} \\ \hat{\mu} &= [\mathbf{a}^T(\hat{\theta})\mathbf{a}(\hat{\theta})]^{-1} \mathbf{a}^T(\hat{\theta})\mathbf{y} \\ \hat{\sigma}^2 &= (mp)^{-1} \mathbf{y}^T P_a^\perp(\hat{\theta})\mathbf{y} \end{aligned} \quad (3.9)$$

where $P_a^\perp(\theta)$ is the complementary projection matrix on the column space of $\mathbf{a}(\theta)$, i.e.,

$$P_a^\perp(\theta) = I - \frac{1}{\|\mathbf{a}(\theta)\|^2} \mathbf{a}(\theta)\mathbf{a}^T(\theta). \quad (3.10)$$

Determination of the ML estimate requires solution of the nonlinear maximization of (3.9). Therefore, it needs reasonable initial conditions. Adequate initial estimates can be obtained by exploiting the parametric model of the concentration distribution. For the quasistatic model, suitable initial values can be obtained using the approach in [11]. For the induced emission scenario, we form the system of nonlinear equations $y(\mathbf{r}_i, t_j) = c(\mathbf{r}_i, t_j)$, where $i = 1, 2, 3$ and j can be chosen arbitrarily. We then obtain an initial estimate for $\hat{\theta}$ by solving this system for the unknown locations.

The Cramér-Rao bound for the unknown parameters can be derived as in [9], resulting in

$$\operatorname{CRB}(\theta) = \frac{\sigma^2}{\mu^2} \{D^T(\theta)P_a^\perp(\theta)D(\theta)\}^{-1} \quad (3.11)$$

$$\operatorname{CRB}(\mu) = \sigma^2 \{\mathbf{a}^T(\theta)P_D(\theta)\mathbf{a}(\theta)\}^{-1} \quad (3.12)$$

$$\operatorname{CRB}(\sigma^2) = \frac{2\sigma^4}{mp} \quad (3.13)$$

where $D(\theta) = \partial\mathbf{a}(\theta)/\partial\theta$: an $(mp \times 3)$ -dimensional matrix.

D. Mine Detection

We define the mine detection problem as a binary decision between two hypothesis: H_0 means that the mine is absent, i.e., $\mu = 0$, and H_1 means that the mine is present, i.e., $\mu > 0$. This formulation can be easily modified for detecting mines with release rates above a certain threshold [13].

We consider a generalized likelihood ratio detector that is most useful when the physical model is reliable and a very effective technique when some parameters in the model are not known [10]. The detector is based on the assumption that the solution (2.7) approximates the physical processes reasonably well and that uncertainties in the model are mainly due to the measurement noise.

Under the above hypotheses and assumptions, the measurement vector is Gaussian distributed: under H_0 , $\mathbf{y} \sim \mathcal{N}[0, \sigma^2 I]$, and under H_1 , $\mathbf{y} \sim \mathcal{N}[\mathbf{a}(\theta)\mu, \sigma^2 I]$.

The GLR test is given by the ratio

$$\operatorname{GLR} = \frac{\sup_{\mu=0, \sigma^2>0} \{l(\mathbf{y}, \theta, \mu)\}}{\sup_{\mu>0, \sigma^2>0} \{l(\mathbf{y}, \theta, \mu)\}} \quad (3.14)$$

where the numerator (denominator) on the r.h.s. corresponds to the maximum likelihood function under H_0 (H_1). The likelihood ratio is then given by

$$\text{GLR} = \left(\frac{\hat{\sigma}_1^2}{\hat{\sigma}_0^2} \right) \quad (3.15)$$

where $\hat{\sigma}_0^2$ and $\hat{\sigma}_1^2$ are the ML estimates of the noise variance under H_0 and H_1 , respectively. These estimates are given by

$$\hat{\sigma}_0^2 = \frac{1}{mp} \mathbf{y}^T \mathbf{y} \quad (3.16)$$

$$\hat{\sigma}_1^2 = \frac{1}{mp} (\mathbf{y} - \mathbf{a}(\hat{\theta})\hat{\mu})^T (\mathbf{y} - \mathbf{a}(\hat{\theta})\hat{\mu}). \quad (3.17)$$

The ML estimate $\hat{\mu}$ of the source intensity under H_1 is computed as [17]

$$\hat{\mu} = \max \left(0, \frac{\mathbf{a}^T(\hat{\theta})\mathbf{y}}{\|\mathbf{a}(\hat{\theta})\|} \right). \quad (3.18)$$

Following the standard approach in the detection literature [16], [18], we determine the threshold τ to yield a desired probability of false alarm P_{fa} (typically $P_{\text{fa}} = 5\%$). Thus, computation of τ requires knowledge of the probability distribution of GLR under H_0 . For small samples, this distribution cannot be computed in closed form due to the nonlinear dependence of $\mathbf{a}(\theta)$ on θ and can only be estimated using Monte Carlo simulations. However, the exact threshold can be computed using the large-sample distribution of the GLR, as we now show.

Let T denote a random variable defined by

$$T = \frac{\mathbf{y}^T P_{\mathbf{a}} \mathbf{y}}{\mathbf{y}^T \mathbf{y}} \quad (3.19)$$

where $P_{\mathbf{a}}$ is the projection matrix on the column space of $\mathbf{a}(\hat{\theta})$. Then, the cumulative distribution of GLR is given by

$$\Pr[\text{GLR} < x] = \Pr[\hat{\mu} > 0] \Pr[T < x]. \quad (3.20)$$

Under the assumption that the product of the numbers of sensors and time samples mp is sufficiently large, we prove, in Appendix A, that the statistical behavior of the statistic T may be characterized by

$$T = \varsigma + \gamma(mp) \quad (3.21)$$

where $\gamma(mp)$ is a random variable such that $mp \cdot \gamma(mp)$ converges in probability to zero, and ς is a random variable whose cumulative distribution function $\Pr[\varsigma \leq x] = W(x, k_1, k_2, \lambda_1, \lambda_2)$ is given by

$$1 - \int_0^\infty (u/(x^{-1} - 1) + 2x\lambda_2/(x^{-1} - 1)^2, k_2 \lambda_2/(x^{-1} - 1)^2) w_\chi(u, k_1, \lambda_1) du \quad (3.22)$$

where

$$\lambda_1 = \mu_0^2 \frac{\mathbf{a}^T(\theta) P_F \mathbf{a}(\theta)}{2\sigma^2}$$

$$\lambda_2 = \mu_0^2 \frac{\mathbf{a}^T(\theta) P_F^\perp \mathbf{a}(\theta)}{2\sigma^2}$$

$$W_\chi(x, k, \lambda) = \int_0^x w_\chi(u, k, \lambda) du$$

$w_\chi(u, k, \lambda)$ = the noncentral chi-square density
function with k degrees of freedom
and noncentrality factor λ (3.23)

and θ_0 and μ_0 denote the true values of the unknown parameters. The matrix P_F is a projection matrix onto the column space of matrix $F(\theta, \mu)$

$$F(\theta, \mu) = [\mu D(\theta) \quad \mathbf{a}(\theta)]. \quad (3.24)$$

Therefore, $mp(T - \varsigma)$ converges in probability to zero as mp tends to infinity. This relatively rapid approach of $(T - \varsigma)$ to zero leads us to expect that the probability $\Pr[\varsigma > \tau]$ would be a good approximation of $\Pr[T > \tau]$ even in relatively small samples, i.e., small mp . The probabilities of detection and false alarm for the GLR detector are given by

$$P_{\text{fa}} = \Pr[\text{GLR} < \tau | H_0] \\ = (1 - \Pr[\hat{\mu} < 0 | H_0]) W(\tau, 4, mp - 4, 0, 0) \quad (3.25)$$

$$P_d = \Pr[\text{GLR} < \tau | H_1] \\ = (1 - \Pr[\hat{\mu} < 0 | H_1]) W(\tau, 4, mp - 4, \lambda_1, \lambda_2) \quad (3.26)$$

where $W(x, 4, mp - 4, \lambda_1, \lambda_2)$ denotes the distribution function of ς ; see (3.22). The expressions for $\Pr[\hat{\mu} < 0 | H_0]$ and $\Pr[\hat{\mu} < 0 | H_1]$ are given in Appendix B.

Numerical evaluation of $\Pr[\varsigma > \tau]$ is done using [19]

$$w_\chi(u, \eta, \lambda) = \sum_{i=0}^{\infty} w_\pi(i, \lambda) w_\chi(u, \eta + 2i, 0) \quad (3.27)$$

where $w_\pi(i, \lambda)$ is the Poisson density function with mean λ .

1) *Mean Detector*: The mean detector makes fewer assumptions about the model than the GLR, and hence, it is useful when a reliable model is not available. In our case, it can be expressed as a test between the following hypotheses: $H_0 - \mathbf{y}$ is distributed as $\mathcal{N}[0, \sigma^2 I]$, and $H_1 - \mathbf{y}$ is distributed as $\mathcal{N}[\xi, \sigma^2 I]$, where ξ is the unknown mean of the measurement, corresponding to concentrations due to the release of explosive vapors from the mine, i.e., $\xi = \mathbf{a}(\theta)\mu$.

This detector is computed using the statistic (see [20, pp. 265–271])

$$T = \frac{1}{mp} \frac{1}{\sqrt{\hat{\sigma}^2}} \sum_{i=1}^{mp} y_i \quad (3.28)$$

where y_i is the i th component of the measurement vector \mathbf{y} , and $\hat{\sigma}^2$ is an estimate of unknown noise variance, which is obtained independently of detection/localization phase.

Under H_0 , T has Student's central t distribution with mp degrees of freedom. Under H_1 , T has a noncentral t distribution with mp degrees of freedom and noncentrality factor $\lambda = ((1/mp) \sum_{i=1}^{mp} \xi_i)^2 / \sigma^2$; see [21]. Therefore, the probabilities of detection and false alarm for this detector are given by

$$P_{\text{fa}} = 1 - \Pr[t_{mp}(0) \leq \tau] \quad (3.29)$$

$$P_d = 1 - \Pr[t_{mp}(\lambda^2) \leq \tau] \quad (3.30)$$

where $t_{mp}(\cdot)$ denotes the cumulative t distribution with mp degrees of freedom and noncentrality factor in parentheses, and τ is the decision threshold.

IV. SENSOR ARRAY DESIGN

In this section, we discuss how to optimally design the array of chemical sensors for estimating the unknown mine location. Our formulation of the design problem includes selection of the array parameters, i.e. number of sensors, number of time samples, and positions of sensors, in order to satisfy a desired criterion. In [13], we derived a design algorithm based on a *detection* performance criterion that can be easily applied to the present problem. Since our current problem also involves estimating the mine location, we propose an alternative design algorithm based on *estimation* performance criteria.

Estimation Performance Criteria

A number of different criteria for evaluating the estimation performance can be used. We will base our criteria on the CRB, which is a universal measure of optimal estimation accuracy. There are various ways to form a scalar criterion using the CRB matrix (3.11), but the two most meaningful choices are i) the trace of $\text{CRB}(\theta)$, which is a measure of the squared magnitude of the location error vector, and ii) the determinant of $\text{CRB}(\theta)$ corresponding to a linearized confidence interval of the location estimate $\hat{\theta}$; see [22].

Thus, using (3.13), we can compute combinations of m and p that give the desired value of the trace or determinant of the CRB matrix. Note that the CRB is a function of the source parameters, mine location, and vapor release rate (or, equivalently, SNR), as well as m and p . Therefore, the values of m and p required to achieve a desired performance also depend on the source parameters. To deal with this dependence on the unknown mine location and source intensity, we assume that *a priori* statistical information on the mine location \mathbf{r}_0 is available, and we implement a Bayesian approach.

Consider, for example, a circular, uniformly spaced sensor array. In this case, the CRB is a function of (m, p, \mathbf{r}_0) only, where we implicitly assume that the array radius is given. Let $m^*(p, \mathbf{r}_0)$ denote the minimum number of sensors required to yield the desired estimation accuracy (the determinant or trace of the CRB matrix) for a given number of snapshots and a given mine location. The optimum number of sensors for the given p is then

$$m_{\text{opt}}(p) = \int_S m^*(p, \mathbf{r}_0) w(\mathbf{r}_0) d\mathbf{r}_0 \quad (4.1)$$

where S is the area being scanned for the presence of mines, and $w(\mathbf{r}_0)$ is the prior density distribution function of the mine location. Repeating this process, we can compute possible combinations $(m_{\text{opt}}(p), p)$ that give the desired estimation accuracy.

Optimum Sensor Positions

We now discuss how to optimally select the positions of the sensors with respect to an arbitrary scalar cost function $C(P_d, \text{CRB})$, which depends on the detection and estimation performance measures P_d and the CRB matrix. The position optimization is useful when the concentration distribution varies with the azimuthal angle, i.e., when the advective diffusion of explosive vapors is non-negligible. Note that we did not include P_{fa} since it does not depend on the sensor locations.

To compute the optimum positions, we exploit the parametric model of the measurement vector and its dependence on the sensor positions.

Assume that the area being checked for the presence of mines is bounded by a certain curve $l(\mathbf{r}) = 0$. Then, we define the optimum sensor positions through the following constrained optimization problem. Let $R = [\mathbf{r}_1 \cdots \mathbf{r}_m]$ be a matrix of sensor positions. The optimum sensor positions R_{opt} are defined by

$$R_{\text{opt}} = \underset{R}{\text{argmin}} C(P_d, \text{CRB}), \quad \text{subject to } l(\mathbf{r}_{i,\text{opt}}) = 0 \quad \text{for } 1 \leq i \leq m \quad (4.2)$$

where we assumed that sensors are located on the perimeter of the region defined by $l(\mathbf{r}_{i,\text{opt}}) = 0$.

To illustrate the proposed approach, consider the following design problem: Find the sensor positions that maximize the detection probability for a fixed false-alarm rate and a given numbers of sensors and time samples. The optimum sensor positions obviously depend on the concentration distribution and unknown mine location. To avoid dependence on the mine location, we use a Bayesian approach, as in the previous section. Suppose, for example, that the area being checked for mines is circular with radius r . Then, the sensor positions are specified by a vector of azimuth angles $\phi = [\phi_1, \dots, \phi_m]^T$. Because the detection probability is a function of azimuth angle due to the noncentrality factor, the optimum vector of azimuth angles ϕ_{opt} is defined as $\phi_{\text{opt}} = \text{argmax } P_d$. Using (3.26), this vector can be numerically computed from the following set of nonlinear equations

$$\frac{\partial \lambda_1}{\partial \phi} \int_{\tau}^{\infty} \frac{\partial w(u, 4, mp - 4, \lambda_1, \lambda_2)}{\partial \lambda_1} du + \frac{\partial \lambda_2}{\partial \phi} \int_{\tau}^{\infty} \frac{\partial w(u, 4, mp - 4, \lambda_1, \lambda_2)}{\partial \lambda_2} du = 0. \quad (4.3)$$

The computational complexity can be greatly reduced by exploiting the fact that the noncentrality factors change slowly with respect to the spatial coordinates, and hence, the partial derivatives $\partial \lambda_1 / \partial \phi$ and $\partial \lambda_2 / \partial \phi$ can be replaced with the first-order approximations.

Then, using ϕ_{opt} computed from (4.3), the optimum locations are given by

$$R_{\text{opt}} = r[\cos(\phi_{\text{opt}}) \sin(\phi_{\text{opt}})]. \quad (4.4)$$

Observe that in the case of negligible advective diffusion, i.e., “weak” wind, the noncentrality factors λ_1 and λ_2 are independent of azimuth angle, i.e., $\partial \lambda_1 / \partial \phi = 0$ and $\partial \lambda_2 / \partial \phi = 0$. Therefore, the sensor locations can be chosen arbitrarily on the area perimeter.

V. MOVING-SENSOR ALGORITHM

We present an algorithm for localizing mines using a moving sensor. This algorithm is of interest for demining since it can be used for remotely controlled guidance of autonomous vehicles (AV's) equipped with chemical sensors, thus avoiding any threat to human life. As shown in [12], a single moving sensor can perform the task of a stationary sensor array by taking measurements at different locations at different times. By exploiting the parametric model (3.2), we can optimize the sensor move-

ment to satisfy certain performance criteria. The optimality criteria used in [12] for planning the sensors' motion is to reduce as much as possible the expected location estimation error after the next measurement is taken. Our goal here is to plan a mobile sensor's trajectory to minimize the time required for it to reach the mine location. We accomplish this goal by computing the estimates of the mine location at each time instance and then moving the sensor toward that location. The important advantage of our algorithm compared with animal-based localization algorithms is the ability to optimally plan sensor's motion in real time to satisfy a desired criterion.

We assume that the time samples are taken uniformly with time interval T_s . The sensor first takes measurements while circling around the area that is being checked for the presence of mines. The proposed algorithm for moving the sensor to find the mine is described by the following steps.

- At each time instance t_j and position \mathbf{r}_j , obtain the measurement $y(\mathbf{r}_j, t_j)$.
- Compute the estimate $\hat{\theta}_j$ using all available measurements $\mathbf{y}_j = [y(\mathbf{r}_1, t_1), \dots, y(\mathbf{r}_j, t_j)]^T$.
- Obtain S_{j+1} , which is the set of all the points reachable by the sensor at time t_{j+1} .
- Move the sensor toward $\hat{\theta}_j$, and repeat the previous steps, or stop the localization algorithm if $\hat{\theta}_j \in S_{j+1}$.

The rationale behind the above algorithm is to choose the point that is closest to the estimated mine location. By repeating this procedure, we expect to minimize the time until the sensor reaches the mine. In addition, by using uniformly spaced, small sampling intervals, we improve the spatial diversity and, hence, the estimation accuracy of our algorithm.

The alternative approach of [12] is based on moving the sensor in the direction of the gradient of the CRB matrix. That algorithm gives a more accurate estimate of the mine location but typically needs a longer time to satisfy the stopping criterion.

VI. NUMERICAL EXAMPLES

We illustrate the applicability of our results by numerical examples. In all examples, unless otherwise stated, we assume a uniformly spaced, circular array with radius $r = 50$ m. We suppose that the measurements are taken every 10 s (starting at $t = 0$) and that the mine is located at $(0, 0)$ at a depth of 10 cm. The release rate was set to 10 mg/s. For this release rate, the concentration of the explosive vapors at the ground level above the mine would be 400 ng/m^3 which is consistent with [23]. We assumed that the advective flow was due to a constant wind velocity of 3 cm/s. The effective diffusivity of explosive vapors in the air was set to $\kappa = 25 \text{ m}^2/\text{s}$, following [24]. Similarly, the effective diffusivity in the ground was set to $\kappa_1 = 10^{-4} \text{ m}^2/\text{s}$; see [25].

A. Concentration Distribution

Fig. 1 illustrates the spatio-temporal evolution of the concentration distribution of explosive vapors in the $z = 0$ plane as a result of a continuous release. In Fig. 2, we show the same result for an impulsive source (remotely induced release) with $\mu = 400 \text{ ng}$.

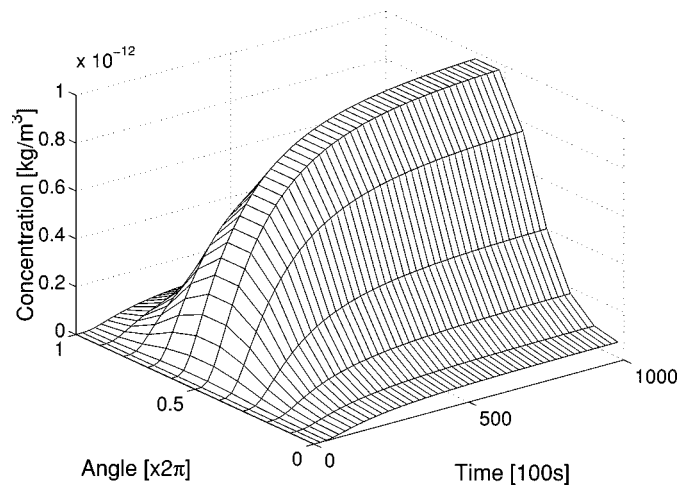


Fig. 1. Concentration distribution at radius $r = 50$ m: continuous source.

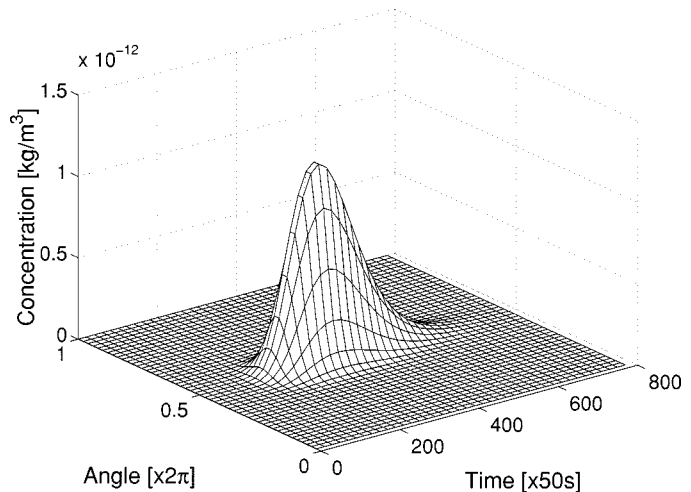


Fig. 2. Concentration distribution at radius $r = 50$ m: induced source.

B. Detection and Estimation Performance

We present numerical examples to demonstrate the performance of both the GLR and mean detectors. In these examples, the thresholds are chosen to yield a 5% probability of false alarm, i.e., $P_{fa} = 0.05$.

In Figs. 3 and 4, we show the probability of detection P_d for the GLR and mean detector, respectively, as a function of the numbers of sensors m and time samples p .

The two most important conclusions from Figs. 3 and 4 are that the detection performance of a mean detector significantly deteriorates compared with the performance of the GLR detector due to absence of a physical model, and for a small number of snapshots, the detection performance will not be significantly improved, even if the number of sensors is large.

To determine the accuracy of the ML estimator, in Fig. 5, we show the square root of $\text{trace}(\text{CRB}(\theta))$ as a function of the number of samples and sensors for fixed $\text{SNR} = 3 \text{ dB}$.

C. Sensor Array Design

Fig. 6 illustrates possible combinations of the numbers of time samples and sensors that yield detection probability $P_d = 95\%$ and $P_{fa} = 0.05$ for the GLR and mean detector. Any point

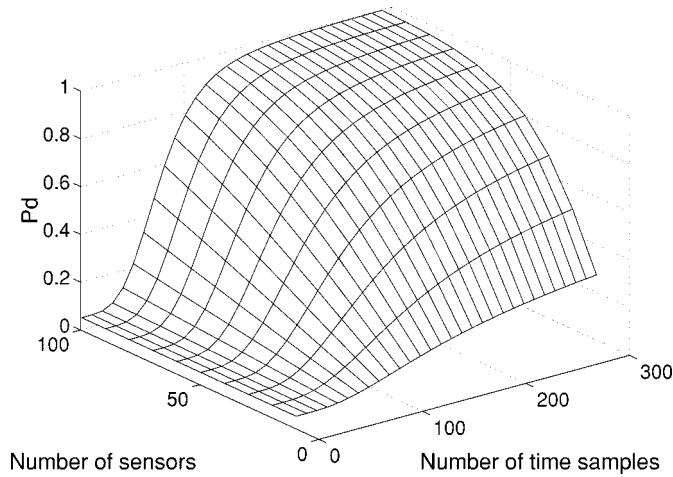


Fig. 3. Detection probability: GLR detector.

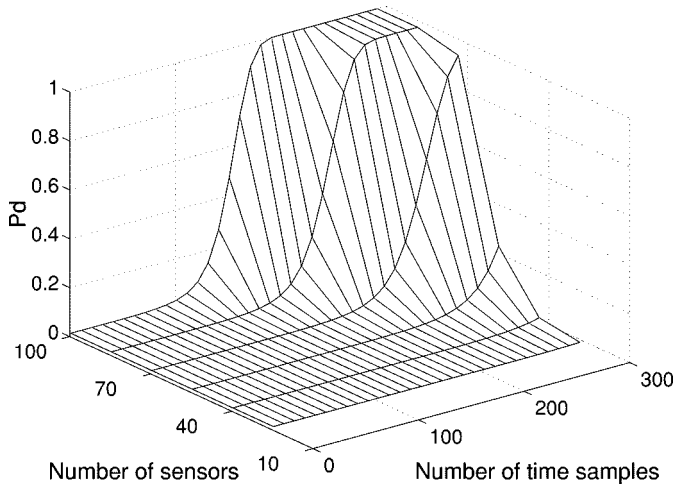


Fig. 4. Detection probability: mean detector.

on the line shown in these figures will guarantee the required P_d and P_{fa} . As expected, the number of time samples required to achieve the same detection performance is significantly larger for the mean detector compared with the GLR detector.

Fig. 7 shows the numbers of sensors and time samples required to ensure that the trace of $\text{CRB}(\theta)$ is smaller than 0.1 m^3 .

D. Moving-Sensor Algorithm

Consider the moving-sensor algorithm from Section V. Assume that the sensor first moves counterclockwise on a circle of radius 50 m centered at $(0,0)$ and starting at time 0. The mine location is set to $(10, 1, -0.1)$. The vehicle's speed is set to 0.2 m/s; see [26]. Measurements are taken every 10 s. At time $t = 350$ s, detection is assumed to have occurred, and then, the localization algorithm begins, initially using the measurements accumulated during the first 350 s. Fig. 8 shows the path traveled by the sensor including the initial circle.

E. Monte-Carlo Comparisons

We examine the adequacy of the large sample approximation by comparing $\text{Pr}[\zeta > \tau]$ with $\text{Pr}[\text{GLR} > \tau]$ for various

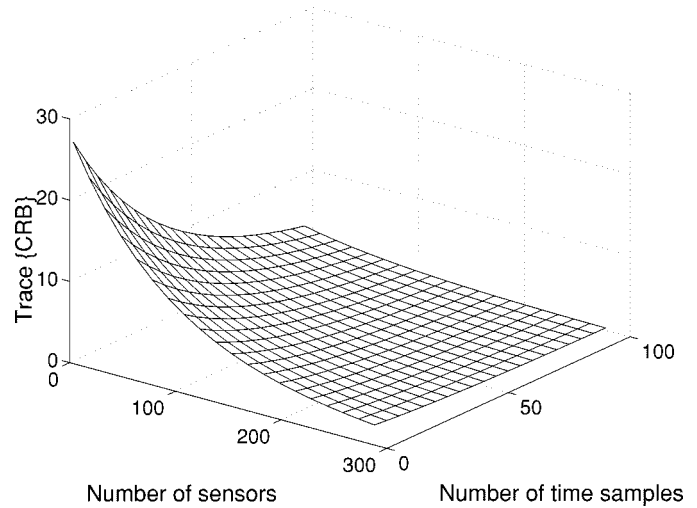


Fig. 5. Trace of CRB (square root).

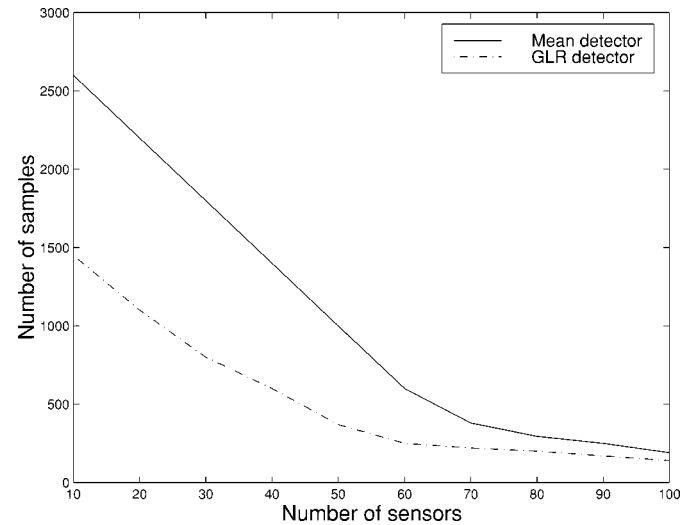


Fig. 6. System parameters to achieve $P_d = 95\%$.

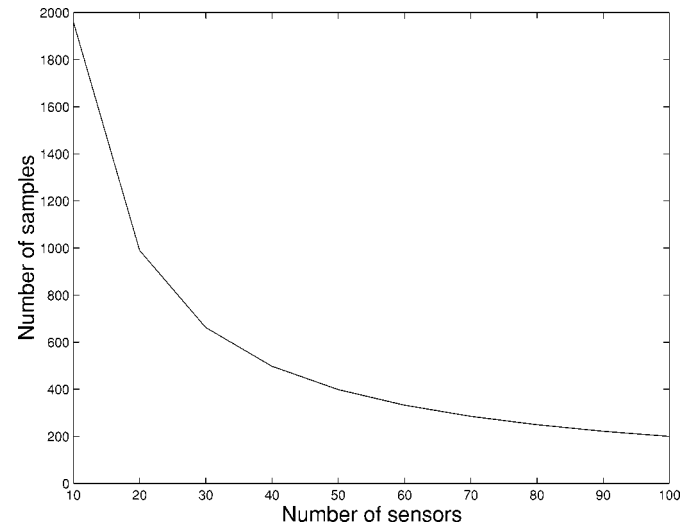


Fig. 7. System parameters to achieve $\text{trace}[\text{CRB}(\theta)] \leq 0.1 \text{ m}^3$.

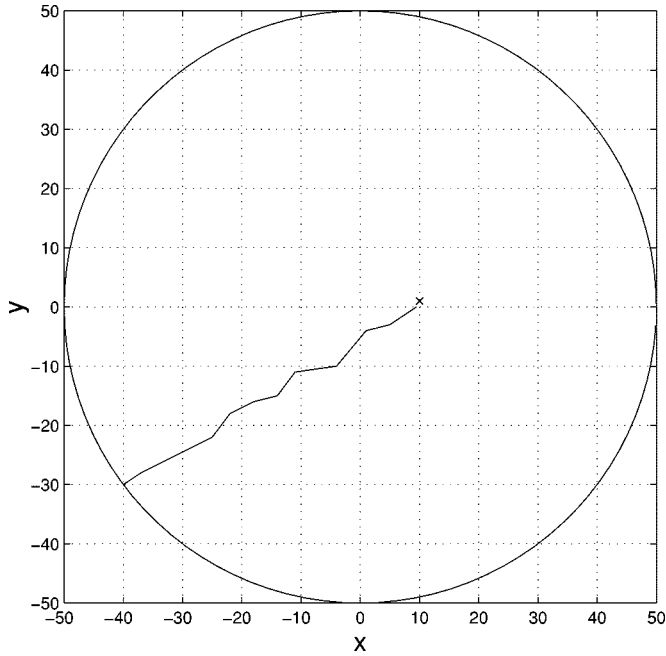


Fig. 8. Sensor's path: moving-sensor algorithm.

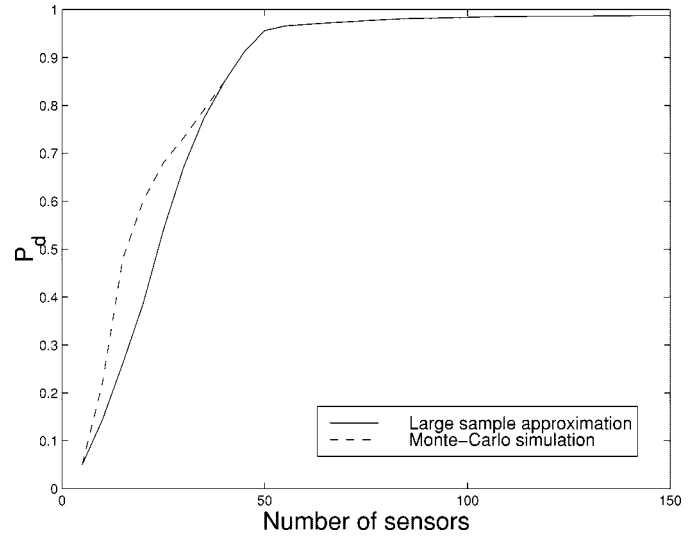
sample sizes. We obtain the concentration distribution using the continuous source model described in Section VI-A. We obtain the measurement vector taking $p = 5$ measurements in steady state. Then we compute the point estimate of $\Pr[\text{GLR} > \tau]$ using 5000 random samples with σ^2 such that $\text{SNR} = 3$ dB. For illustrational purposes, we select τ such that $P_{\text{fa}} = 0.05$ for $m = 100$. In Fig. 9, we present probabilities $\Pr[X > \tau]$ and $\Pr[\text{GLR} > \tau]$ as a function of number of sensors m . The small difference between the empirical distribution and the large sample approximation in Fig. 9 supports the use of the large sample approximation for this threshold, although we must always be wary in generalizing Monte Carlo studies.

VII. DISTRIBUTED SOURCE

In this section, we discuss a possible extension of the proposed techniques to the case of a distributed source. The single point source model discussed earlier may not be a valid approximation if the distances between sensors and source are not sufficiently large. Thus, we are motivated to use a more realistic distributed source model of unknown shape that incorporates the effect of finite source dimensions.

First, we derive a physical model (spatio-temporal evolution of the concentration distribution) amenable to statistical signal processing techniques. The most general model of the distributed source assumes unknown release rate both in space and time $\mu(\mathbf{r}, t)$. The estimation of fully unknown $\mu(\mathbf{r}, t)$ is obviously an ill-posed problem since it cannot be uniquely determined from a finite set of spatio-temporal measurements. Therefore, we propose to approximate the release rate $\mu(\mathbf{r}, t)$ using a basis function model

$$\mu(\mathbf{r}, t) = \sum_{l=1}^{n_b} \mu_l \psi_l(\mathbf{r}, t) \quad (7.1)$$


 Fig. 9. Detection probability for five time samples and $P_{\text{fa}} = 5\%$.

where $\{\psi_l(\mathbf{r}, t), l = 1, n_b\}$ is a set of *a priori* known spatial and temporal basis functions, n_b is the number of basis functions, and μ_l are the unknown basis function coefficients.

Let $h(\mathbf{r}, \mathbf{r}_0, t)$ denote the concentration at the location \mathbf{r} and time t due to an instantaneous release of vapor from a source located at \mathbf{r}_0 . The concentration distribution is then given by

$$c(\mathbf{r}, t) = \sum_{l=1}^{n_b} \mu_l \int \psi_l(\mathbf{r}_0, t) h(\mathbf{r}, \mathbf{r}_0, t) d\mathbf{r}_0. \quad (7.2)$$

The corresponding statistical model is given by

$$\mathbf{y} = A\boldsymbol{\mu} + \mathbf{e} \quad (7.3)$$

where A is an $(mp \times n_b)$ -dimensional source-to-sensor transfer matrix, $\boldsymbol{\mu}$ is the n_b -dimensional vector of unknown basis function coefficients $\boldsymbol{\mu} = [\mu_1, \dots, \mu_{n_b}]^T$, and the remaining notation is the same as in Section III-A. Note that we have omitted dependence of $c(\mathbf{r}, t)$ on θ since (7.2) depends on environmental parameters only, which are assumed to be known.

We formulate the detection of a distributed source as a binary decision between two hypothesis: H_0 means the source is absent, i.e., $\boldsymbol{\mu} = \mathbf{0}$, and H_1 means the source is present, i.e., $\mu_l > 0$ for at least one l . We showed in [13] that in this case, the GLR test has an F -distribution: central under H_0 and noncentral under H_1 . Thus, the performance of this detector is given by

$$P_{\text{fa}} = 1 - \Pr[F_{n_b, mp-n_b}(0) > \tau] \quad (7.4)$$

$$P_{\text{fa}} = 1 - \Pr[F_{n_b, mp-n_b}(\lambda) > \tau] \quad (7.5)$$

$$\lambda = \frac{1}{\sigma^2} \boldsymbol{\mu}^T A^T A \boldsymbol{\mu} \quad (7.6)$$

where τ is the decision threshold.

VIII. CONCLUDING REMARKS

We have proposed methods for localizing and detecting landmines using chemical sensor arrays and optimum statistical signal processing. The methods are parametric, being based on physical modeling of the spatial and temporal distributions of the explosive vapors released from the buried mines. The

proposed parametric model was obtained by solving the diffusion equation for the given boundary conditions. We based the localization algorithm on the maximum likelihood estimate. The detection algorithm included the GLR and mean detector. The GLR detector gives a higher performance and is applicable when the physical model is reliable, whereas the mean detector is useful when a precise model is not available. We have analyzed the performance of both detectors using the probability of detection P_d and false alarm P_{fa} .

We presented algorithms for optimal array design for various performance measures. The design included selecting the number of sensors and time samples. We also developed an algorithm for mine localization using a moving sensor. The proposed algorithm allows real-time optimization of the sensor's trajectory and typically minimizes the time needed to reach the mine. Numerical simulations demonstrated the applicability of our results.

Future research will include improving the detection and estimation performance using flux measurements and dealing with multiple mines and nonselective sensors. The expression (3.26) was derived under the assumption that the sensor noise can be modeled as Gaussian. Research should be undertaken to investigate changes in detection performance and array design in order to develop more realistic noise and environment models. Finally, an effort should be made to examine the proposed algorithms' robustness against modeling errors.

APPENDIX A STATISTICAL BEHAVIOR OF GLR

In this Appendix, we derive the distribution function of the likelihood ratio statistic under the large-sample assumption. The ML estimate of noise variance under H_1 is given by [19]

$$\hat{\sigma}_1^2 = \frac{1}{mp} \mathbf{e}^T P_F^\perp \mathbf{e} + \gamma(mp). \quad (\text{A.1})$$

Then, the likelihood ratio statistic is given by

$$\begin{aligned} T(\mathbf{y}) &= \frac{\mathbf{e}^T P_F^\perp \mathbf{e}}{\mathbf{e}^T \mathbf{e}} + \gamma(mp) \\ &= \frac{\mathbf{e}^T P_F^\perp \mathbf{e}}{(\mathbf{e} + \mathbf{a}(\theta_0)\mu_0)^T (\mathbf{e} + \mathbf{a}(\theta_0)\mu_0)} + \psi(mp) \\ &= \varsigma + \psi(mp) \end{aligned} \quad (\text{A.2})$$

where θ_0 and μ_0 denote true values, and $\psi(mp) = (1/mp)\gamma(mp)/\mathbf{e}^T \mathbf{e}$. The random variable $mp \cdot \psi(mp)$ converges in probability to zero since $(1/mp)\mathbf{e}^T \mathbf{e}$ converges in probability to σ_0^2 by the strong law of large numbers.

Let $\mathbf{z} = \sigma^{-1}\mathbf{e}$ and $\mathbf{u} = \sigma^{-1}\mathbf{a}(\theta_0)\mu_0$. The cumulative distribution function of GLR is given by $\Pr[\varsigma \leq x] = \Pr[\mathbf{z}^T P_F^\perp \mathbf{z} < x(\mathbf{z} + \mathbf{u})^T (\mathbf{z} + \mathbf{u})]$. The random variable \mathbf{z} is Gaussian distributed and has a diagonal covariance matrix. For an arbitrary constant ξ , the random variable $(\mathbf{z} + \xi\mathbf{u})^T P_F (\mathbf{z} + \xi\mathbf{u})$ has a noncentral chi-square distribution with $\text{rank}(P_F)$ degrees of freedom and noncentrality factor $\xi^2(\mathbf{u}^T P_F \mathbf{u}/2)$ since P_F is a projection matrix and, hence, idempotent. Similarly, $(\mathbf{z} + \xi\mathbf{u})^T P_F^\perp (\mathbf{z} + \xi\mathbf{u})$ has a noncentral chi-squared distribution with $mp - \text{rank}(P_F)$ degrees of freedom and noncentrality factor $\xi^2(\mathbf{u}^T P_F^\perp \mathbf{u}/2)$. The

random variables $\mathbf{z}^T P_F^\perp \mathbf{z}$ and $(\mathbf{z} + \mathbf{u})^T (\mathbf{z} + \mathbf{u})$ are obviously dependent, and thus, to compute the distribution function first, we rewrite $(\mathbf{z} + \mathbf{u})^T (\mathbf{z} + \mathbf{u})$ as a sum of two independent random variables $(\mathbf{z} + \mathbf{u})^T P_F (\mathbf{z} + \mathbf{u})$ and $(\mathbf{z} + \mathbf{u})^T P_F^\perp (\mathbf{z} + \mathbf{u})$.

To simplify computations, let us introduce $Q(x) = \Pr[1/\varsigma < x]$. The distribution function of ς is then given by $\Pr[\varsigma < x] = 1 - Q(x^{-1})$.

For $\xi > 0$, the cumulative distribution function of $1/\varsigma$ can be computed as

$$\begin{aligned} \Pr[1/\varsigma < \xi + 1] &= \Pr[(\mathbf{z} + \mathbf{u})^T P_F (\mathbf{z} + \mathbf{u}) \\ &> \xi(\mathbf{z} - \xi^{-1}\mathbf{u})^T P_F^\perp (\mathbf{z} - \xi^{-1}\mathbf{u}) \\ &\quad - (1 + \xi^{-1})\mathbf{u}^T P_F^\perp \mathbf{u}]. \end{aligned} \quad (\text{A.3})$$

Let $s_1 = (\mathbf{z} + \mathbf{u})^T P_F (\mathbf{z} + \mathbf{u})$ and $s_2 = \xi(\mathbf{z} - \xi^{-1}\mathbf{u})^T P_F^\perp (\mathbf{z} - \xi^{-1}\mathbf{u})$; then, using

$$\Pr[s_1 > s_2 - c] = \int_0^\infty w_{s_1}(x_1) dx_1 \int_0^{s_1+c} w_{s_2}(x_2) dx_2 \quad (\text{A.4})$$

we obtain

$$\begin{aligned} \Pr[1/\varsigma < \xi + 1] &= \int_0^\infty w_\chi(x, \text{rank}(P_F), \lambda_1) \\ &\quad \cdot W_\chi(x/\xi + (\xi + 1)\lambda_2/\xi^2, \\ &\quad mp - \text{rank}(P_F), \lambda_2/\xi^2) \cdot dx \end{aligned} \quad (\text{A.5})$$

where

$$\begin{aligned} \lambda_1 &= \mathbf{u}^T P_F \mathbf{u}/2, \\ \lambda_2 &= \mathbf{u}^T P_F^\perp \mathbf{u}/2. \end{aligned} \quad (\text{A.6})$$

Using the substitution

$$x = (\xi + 1)^{-1}. \quad (\text{A.7})$$

we obtain the distribution function (3.22).

APPENDIX B COMPUTATION OF $\Pr[\hat{\mu} < 0]$

We compute the probability $\Pr[\hat{\mu} < 0]$ under H_0 and H_1 .

The statistical behavior of the ML estimates $\hat{\theta}$ and $\hat{\mu}$ is given by [27]

$$\begin{aligned} \begin{bmatrix} \hat{\theta} \\ \hat{\mu} \end{bmatrix} &= \begin{bmatrix} \theta_0 \\ \mu_0 \end{bmatrix} + \begin{bmatrix} D^T(\theta_0)D(\theta_0) & D^T(\theta_0)\mathbf{a}(\theta_0) \\ \mathbf{a}^T(\theta_0)D(\theta_0) & \mathbf{a}^T(\theta_0)\mathbf{a}(\theta_0) \end{bmatrix}^{-1} \\ &\quad \times \begin{bmatrix} D^T(\theta_0) \\ \mathbf{a}^T(\theta_0) \end{bmatrix} \mathbf{e} + o(1/\sqrt{mp}) \end{aligned} \quad (\text{B.1})$$

where $o(1/\sqrt{mp})$ is a random variable such that $\sqrt{mp} \cdot o(1/\sqrt{mp})$ converges in probability to zero. By applying block inversion to (B.1) and under large sample assumption, we obtain

$$\hat{\mu} = \mu_0 + \frac{\mathbf{a}^T P_D^\perp \mathbf{e}}{\mathbf{a}^T P_D^\perp \mathbf{a}} \quad (\text{B.2})$$

where we omitted dependence on θ_0 and μ_0 . Therefore, the ML estimate $\hat{\mu}$ is Gaussian distributed with mean μ_0 and variance

$$\sigma_\mu^2 = \sigma^2 (\mathbf{a}^T P_D^\perp \mathbf{a})^{-1}. \quad (\text{B.3})$$

Then, the probabilities $\Pr[\hat{J}_l < 0]$ under H_0 and H_1 are given by

$$\Pr[\hat{J}_l < 0 | H_0] = 0.5 \quad (\text{B.4})$$

$$\Pr[\hat{J}_l < 0 | H_1] = \text{erfc}(\mu_{l0}/\sqrt{2}\sigma_{\mu}). \quad (\text{B.5})$$

REFERENCES

- [1] "Sensor technology assessment for ordnance and explosive waste detection and location," Jet Propulsion Lab., Pasadena, CA, JPL D-11 367 rev. B, Mar. 1995.
- [2] C. Bruschini and B. Gros, "A survey of current sensor technology research for the detection of landmines," in *Proc. SusDem*, Zagreb, Croatia, Sept. 1997, pp. 618–627.
- [3] D. L. Patel, "Best type of sensors for the detection of buried mines," in *Proc. Autonomous Veh. Mine Countermeas. Symp.*, Monterey, CA, Apr. 1995, pp. 648–659.
- [4] K. Tsipis, "Landmine Brainstorming Workshop," Program Sci. Technol. Int. Security, Cambridge, MA, Rep. 27, 1996.
- [5] S. A. Brink, "Bofors Schnauzer—A biosensor for detection of explosives," in *Proc. EUREL Conf.*, Edinburgh, U.K., Oct. 1996, pp. 33–36.
- [6] A. Jeremić and A. Nehorai, "Mine detection and localization using chemical sensor array processing," in *Proc. SPIE Detection Remediation Technol. Mines Minelike Targets IV*, Orlando, FL, Apr. 1999.
- [7] —, "Landmine detection and localization using chemical sensor array processing," Dept. Elect. Eng. Comput. Sci., Univ. Illinois, Chicago, IL, Rep. UIC-EECS-99-4, June 1999.
- [8] T. R. Consi, J. Atema, C. A. Goudey, J. Cho, and C. Chryssostomidis, "AUV guidance with chemical signals," in *Proc. IEEE Symp. Autonomous Underwater Veh. Technol.*, Cambridge, MA, July 1994, pp. 450–452.
- [9] P. Stoica and A. Nehorai, "MUSIC, maximum likelihood, and Cramér-Rao bound," *IEEE Trans. Signal Processing*, vol. 37, pp. 720–738, May 1989.
- [10] T. W. Anderson, *An Introduction to Multivariate Statistical Analysis*. New York: Wiley, 1984.
- [11] A. Nehorai, B. Porat, and E. Paldi, "Detection and localization of vapor-emitting sources," *IEEE Trans. Signal Processing*, vol. 43, pp. 243–253, Jan. 1995.
- [12] B. Porat and A. Nehorai, "Localizing vapor-emitting sources by moving sensors," *IEEE Trans. Signal Processing*, vol. 44, pp. 1018–1021, Apr. 1996.
- [13] A. Jeremić and A. Nehorai, "Design of chemical sensor arrays for monitoring disposal sites on the ocean floor," *IEEE J. Oceanic Eng.*, vol. 23, pp. 334–343, Oct. 1998.
- [14] R. P. Muramann, Y. Nakano, T. J. Simpson, D. C. Legett, and D. M. Anderson, "Influence of soil on detection of buried explosives tunnels by trace gas analysis," AD757667, U.S. Cold Reg. Res. Eng. Lab. Rep.
- [15] P. V. Tsoi, "Heat exchange in a system of bodies during unsteady conditions," *IFZh*, vol. IV, no. 1, pp. 120–123, 1961.
- [16] H. L. Van Trees, *Detection, Estimation, and Modulation Theory; Part I*. New York: Wiley, 1968.
- [17] C. L. Lawson and R. J. Hanson, *Solving Least Squares Problems*. Englewood Cliffs, NJ: Prentice-Hall, 1974.
- [18] H. V. Poor, *An Introduction to Signal Detection and Estimation*. New York: Springer-Verlag, 1994.
- [19] F. A. Graybill, *An Introduction to Linear Statistical Models*. New York: Mc Graw-Hill, 1961, vol. I.
- [20] J. C. Kiefer, *Introduction to Statistical Inference*. New York: Springer-Verlag, 1987.
- [21] C. R. Rao, *Linear Statistical Inference and Its Applications*. New York: Wiley, 1973.
- [22] A. Dogandžić and A. Nehorai, "Localization of evoked electric sources and design of EEG/MEG sensor arrays," in *Proc. 9th IEEE SP Workshop Stat. Signal Array Process.*, Portland, OR, Sept. 1998, pp. 228–231.
- [23] J. E. McFee and Y. Das, "The detection of buried explosive objects," *Can. J. Remote Sensing*, vol. 6, pp. 104–121, Dec. 1980.
- [24] W. M. Rohsenow and H. Choi, *Heat Mass and Momentum Transfer*. Englewood Cliffs, NJ: Prentice-Hall, 1961.
- [25] I. N. Nassar and R. Horton, "Heat, water, and solute transfer in unsaturated porous media. Theory development and transport coefficient evaluation," *Transport Porous Media*, vol. 27, pp. 17–38, Apr. 1997.
- [26] A. J. Healy, S. McMillan, D. Jenkins, and R. B. McGhee, "BUGS: Basic UXO gathering system," in *Proc. Autonomous Veh. Mine Countermeas. Symp.*, Monterey, CA, Apr. 1995.
- [27] R. A. Gallant, *Nonlinear Statistical Models*. New York: Wiley, 1987.

Aleksandar Jeremić (S'97) received the B.Sc. degree in electrical engineering from the University of Belgrade, Belgrade, Yugoslavia, in 1995 and M.Sc. degree in electrical engineering from the University of Illinois at Chicago in 1997. Currently, he is pursuing the Ph.D. degree with the Department of Electrical Engineering and Computer Science, University of Illinois at Chicago.

Arye Nehorai (S'80–M'83–SM'90–F'94) received the B.Sc. and M.Sc. degrees in electrical engineering from the Technion—Israel Institute of Technology, Haifa, in 1976 and 1979, respectively, and the Ph.D. degree in electrical engineering from Stanford University, Stanford, CA, in 1983.

After graduation, he worked as a Research Engineer for Systems Control Technology, Inc., Palo Alto, CA. From 1985 to 1995, he was with the Department of Electrical Engineering, Yale University, New Haven, CT, where he became an Associate Professor in 1989. In 1995, he joined the Department of Electrical Engineering and Computer Science, The University of Illinois at Chicago (UIC), as a Full Professor. He holds a joint professorship with the Bioengineering Department at UIC. His research interests are in signal processing, communications, and biomedicine.

Dr. Nehorai is the Editor-in-Chief of the IEEE TRANSACTIONS ON SIGNAL PROCESSING, an Associate Editor of IEEE SIGNAL PROCESSING LETTERS, the IEEE JOURNAL OF OCEANIC ENGINEERING, of *Circuits, Systems, and Signal Processing*, and *The Journal of the Franklin Institute*. He is also a Member of the Editorial Board of *Signal Processing* and has previously been an Associate Editor of the IEEE TRANSACTIONS ON ACOUSTICS, SPEECH, AND SIGNAL PROCESSING, and IEEE TRANSACTIONS ON ANTENNAS AND PROPAGATION. He served as Chairman of the Connecticut IEEE Signal Processing Chapter from 1986 to 1995 and is currently a founding member and the Vice-Chair of the IEEE Signal Processing Society's Technical Committee on Sensor Array and Multichannel (SAM) Processing. He is the co-General Chair of the First IEEE SAM Signal Processing Workshop to be held in 2000. In 1979 and 1980, he received the Rothschild Fellowship in science and engineering, which is awarded annually to eight new graduates throughout Israel. He was co-recipient, with P. Stoica, of the 1989 IEEE Signal Processing Society's Senior Award for Best Paper. He has been a Fellow of the Royal Statistical Society since 1996.